

## Activation enthalpies for oxygen ion motion in cubic yttria-stabilized zirconia

R. J. Darby · R. V. Kumar

Received: 16 June 2008 / Accepted: 2 September 2008 / Published online: 19 September 2008  
© Springer Science+Business Media, LLC 2008

### Introduction

The high oxygen ion conductivity of the yttria-stabilized zirconia (YSZ) system is well known. The conductivity at 1000 °C increases with YO<sub>1.5</sub> addition to around 15–18 mol.% YO<sub>1.5</sub>, when the dopant content is just sufficient to fully stabilize the cubic fluorite phase. Further yttria additions result in a decrease in the conductivity [1, 2]. There are several contributory factors suggested to explain the conductivity decrease: formation of defect clusters reducing oxygen vacancy mobility [3–5], hindrance of oxygen ion motion due to the increasing presence of ‘large’ yttrium ions [6–8], and the increasing presence of a grain boundary phase [9]. Support for the influence of defect clusters is the observation that the activation enthalpy for oxygen ion conduction decreases at high temperatures (decreasing by ~0.2 eV above ~650 °C for 15 mol.% YO<sub>1.5</sub>) [4, 10, 11]. This has been correlated with the breaking-up of short-range order [11].

Although there is a wide compositional range of cubic stability, only a few studies have experimentally investigated yttria contents above 33 mol.% YO<sub>1.5</sub> [12–15]. In these studies the activation enthalpy was observed to increase with yttria content until ~33 mol.% YO<sub>1.5</sub> where the activation enthalpy ‘saturated’ to a value of ~1.3 eV. The authors are unaware of any comment made so far on this saturation effect and it is thus the focus of this letter, allowing an insight into the different contributions to the conductivity decline.

Powders containing between 21 and 53 mol.% YO<sub>1.5</sub> were prepared via roll-milling 8 mol.% Y<sub>2</sub>O<sub>3</sub>-stabilized zirconia powder (TZ-8Y, Tosoh Corporation) with additional yttria powder (99.99% purity, Sigma–Aldrich) in ethanol for 24 h. These powders were subsequently calcined at 900 °C for 4 h, pressed into cuboids or pellets and then sintered at 1500 °C for 48 h in air. Platinum electrodes (Platinum Ink 6926, Metalor) were applied to the faces of the samples for the conductivity measurements. All samples were confirmed to possess the cubic fluorite structure via X-ray diffraction and Raman spectroscopy and had relative densities of over 95%. Both ac impedance and 4-point dc measurements were made using a Solartron 1260 frequency response analyser coupled with a Solartron 1287 potentiostat.

When possible, the conductivity of each of the samples was measured by the 4-point dc method between ~480 and 1000 °C (Fig. 1). The variation of conductivity with composition agrees with previous work, decreasing with an increasing yttria content.

The variation of conductivity,  $\sigma$ , with temperature,  $T$ , is given in an Arrhenius form by:

$$\ln \sigma T = \frac{\Delta H^*}{k_B T} + \ln A, \quad (1)$$

where  $\Delta H^*$  is the activation enthalpy,  $k_B$  the Boltzmann constant and  $A$  is known as the pre-exponential factor. Using the gradients in Fig. 1 along with (1) it is possible to determine the activation enthalpy for each sample.

As previously stated, it is known that the Arrhenius plots display a temperature-dependent gradient for low yttria contents. Temperature-dependent gradients have previously been observed up to ~38 mol.% YO<sub>1.5</sub> [16]. All the samples measured here display such a temperature-dependent gradient. This is illustrated by the highest yttria

R. J. Darby (✉) · R. V. Kumar  
Department of Materials Science and Metallurgy,  
University of Cambridge, Cambridge, UK  
e-mail: rjd44@cam.ac.uk

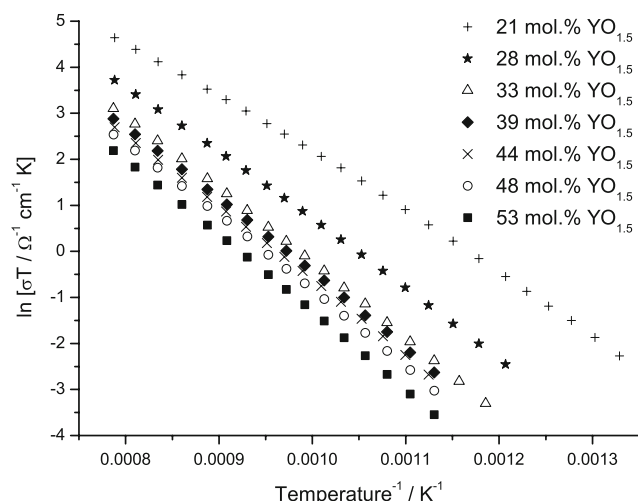


**Fig. 1** The variation of total conductivity, measured by the 4-point dc method, with temperature for a range of samples within the cubic phase-field of the YSZ system

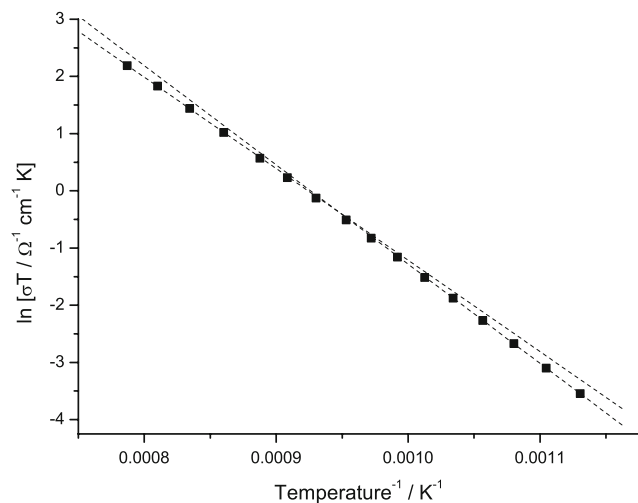


**Fig. 2** Detail of the total conductivity variation, measured by the 4-point dc method, with temperature for the 53 mol.%  $\text{YO}_{1.5}$  sample. Two separate linear fits are used for the high- and low-temperature regions

content sample tested, 53 mol.%  $\text{YO}_{1.5}$  (Fig. 2). Although two linear fits have been used to analyse the data, it must be emphasized that this does not necessarily indicate that there are two distinct regions of behaviour with an intermediate transition temperature. Such analysis, using two linear fits, has been common in the past [4, 10, 11], but recent work has clearly illustrated the activation enthalpy continuously changing with temperature [16].

Activation enthalpies for all samples were calculated in the lowest temperature range where data were obtained for all samples, between 610 and 675 °C, as well as the highest temperature region measured, between 890 and 1000 °C (Fig. 3). The difference between the low temperature and

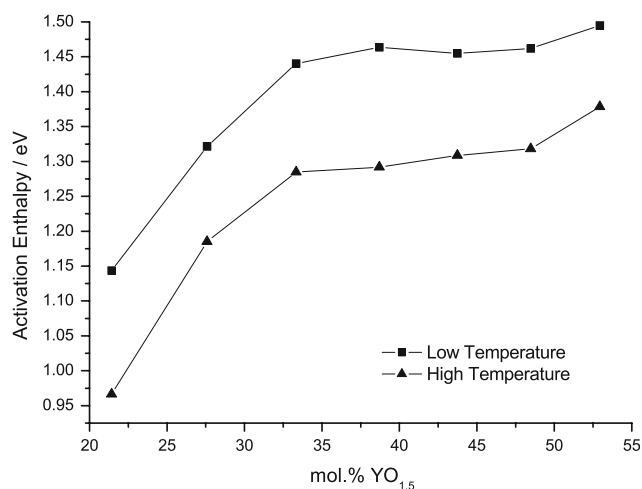


**Fig. 3** Variation of the activation enthalpies with yttria content within the cubic region of the YSZ system

high temperature activation enthalpies is remarkably constant, varying between 0.12 and 0.18 eV. As the activation enthalpy decrease has been correlated with the removal of short-range order in the low yttria content samples, it can be suggested that these higher yttria content samples are undergoing a similar dissociation of defect clusters [11]. This results in the similar reduction in activation enthalpy.

The activation enthalpy for oxygen ion motion is composed of two contributions; a migrational enthalpy,  $\Delta H_m$ , and an association enthalpy,  $\Delta H_a$  [17]:

$$\Delta H^* = \Delta H_m + \Delta H_a. \quad (2)$$

The migrational enthalpy represents the energy barrier between adjacent oxygen ion sites while the association enthalpy accounts for such interactions that introduce short-range ordering (such as between the relatively negatively charged dopant cation and positively charged oxygen vacancy as well as the lattice relaxation accommodating the differently sized dopant). These interactions must be overcome to mobilize oxygen ions and vacancies for conduction. Variation in either the migrational enthalpy, association enthalpy or both may account for the compositional variation in the activation enthalpy observed here.

Lee and Navrotsky [18, 19] have recently reported enthalpy of formation data for the YSZ system that will aid the interpretation of the relative contributions of the different enthalpies in (2). From these data it is possible to calculate the enthalpy of mixing,  $\Delta H_{\text{mix}}$ , which is the deviation from a linear variation between the end-members (Fig. 4). The end-members are the enthalpy for the transition between the stable low-temperature monoclinic phase of zirconia and cubic fluorite zirconia,  $\Delta H_{\text{m} \rightarrow \text{c}}^{\text{ZrO}_2}$ , and the transition of the stable low-temperature C-type cubic yttria to cubic fluorite yttria,  $\Delta H_{\text{C} \rightarrow \text{c}}^{\text{YO}_{1.5}}$ . The negative

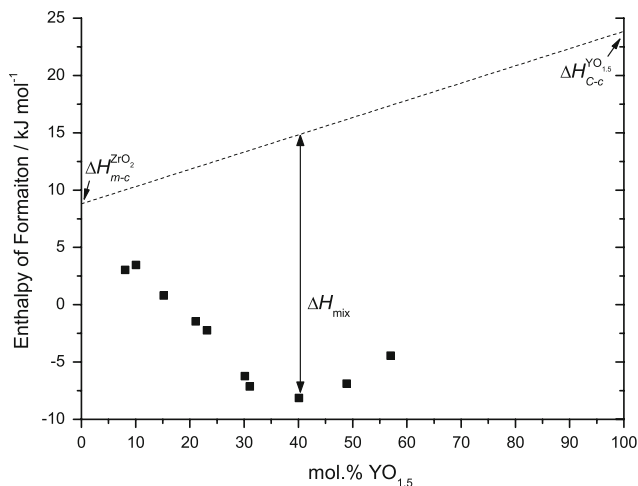


**Fig. 4** Enthalpy of formation data for the YSZ system from [18, 19]. The deviation from the linear ‘ideal solution’ line represents the enthalpy of mixing

deviation from the linear line suggests favourable interactions. Such interactions are responsible for the association enthalpy term in (2).

In order to understand how the variation in the enthalpy of mixing is affecting the interactions experienced by each oxygen vacancy, the data are normalized relative to the number of oxygen vacancies present (Fig. 5). This shows that additional oxygen vacancies experience a similar amount of interactions below ~30 mol.% YO<sub>1.5</sub>, represented by a relatively constant enthalpy of mixing per oxygen vacancy with increasing yttria content. Thus it can be inferred that the association enthalpy term in (2) is constant below ~30 mol.% YO<sub>1.5</sub>. The activation enthalpy variation in this composition range must be entirely due to an increasing migrational enthalpy with yttria content.

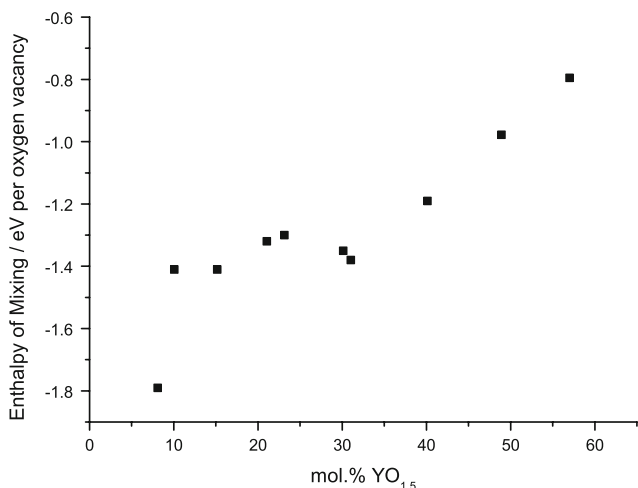


**Fig. 5** Variation in the enthalpy of mixing, normalized to the number of oxygen vacancies present, in the YSZ system

An increase in migrational enthalpy would be expected with increasing yttria content as it results in an increasing presence of larger yttrium ions, sterically hindering the motion of oxygen ions (the zirconium and yttrium ions have ionic radii of 0.84 and 1.019 Å, respectively [20]). Thus the activation enthalpy is initially increasing with yttria content due to the increased likelihood of a mobile oxygen ion having to pass a large yttrium ion. This observation of a ‘blocking effect’ is in agreement with computer simulations [6–8]. In particular it corroborates the conclusions of a recent analytical model of YSZ conductivity by Martin [21]. Martin found that the variation in conductivity with dopant content was best modelled by a constant favourable enthalpy of association coupled with an increasing amount of blocking caused by the increasing proportion of large yttrium ions. This is exactly what has been experimentally observed here for samples with yttria contents below ~30 mol.% YO<sub>1.5</sub>.

Beyond ~30 mol.% YO<sub>1.5</sub>, the enthalpy of mixing per oxygen vacancy becomes less exothermic, suggesting fewer favourable interactions (possibly due to the increasing presence of yttrium ions and oxygen vacancies beginning to interact repulsively, coupled with increasing amounts of strain). This indicates that the association enthalpy contribution in (2) is becoming less with further yttria additions. The migrational enthalpy term will keep increasing due to the increasing presence of relatively large yttrium ions. An increasing ΔH<sub>m</sub> and a decreasing ΔH<sub>a</sub> result in the almost constant activation enthalpy observed in this composition range.

A further increase in the activation enthalpy is observed for the 53 mol.% YO<sub>1.5</sub> sample. As the association enthalpy is continuing to decrease this must be due to a greater increase in the migrational enthalpy as more than half the cation sites are now occupied by large yttrium ions.

Overall the activation enthalpy variation with yttria content has been explained in terms of the migrational and association enthalpy contributions. At low yttria contents (below ~30 mol.% YO<sub>1.5</sub>) the activation enthalpy increases due to an increasing migrational enthalpy term, caused by the increasing presence of large yttrium ions. The association enthalpy is constant in this region as each defect cluster is relatively isolated, the additional oxygen vacancies created on yttria addition are thus in similar environments and are similarly ‘associated’. At high yttria contents (beyond ~30 mol.% YO<sub>1.5</sub>) the defect clusters are no longer isolated and begin to interact, becoming destabilized and reducing the association enthalpy. The migrational enthalpy keeps increasing resulting in the saturation of the activation enthalpy observed.

As the activation enthalpy is the dominant factor affecting the measured conductivity value [22], this analysis suggests that the sudden conductivity decrease beyond

the yttria content required for cubic stabilization is caused by an increasing amount of large yttrium ions in the zirconia matrix. It is not caused by an increasing amount of defect cluster formation. For completeness the suggestion that the conductivity decreases due to the increasing presence of a grain boundary phase was investigated by impedance spectroscopy. No such additional contribution to the conductivity at higher yttria contents was observed.

**Acknowledgements** R.J.D. and R.V.K. would like to thank Ian Farnan for helpful discussions. R.J.D. acknowledges funding from UK Engineering and Physical Sciences Research Council.

## References

1. Badwal SPS (1992) *Solid State Ionics* 52:23. doi:[10.1016/0167-2738\(92\)90088-7](https://doi.org/10.1016/0167-2738(92)90088-7)
2. Hattori M, Takeda Y, Sakaki Y, Nakanishi A, Ohara S, Mukai K et al (2004) *J Power Sources* 126:23. doi:[10.1016/j.jpowsour.2003.08.018](https://doi.org/10.1016/j.jpowsour.2003.08.018)
3. Kilner JA, Steele BCH (1981) In: Sørensen OT (ed) *Mass transport in anion-deficient fluorite oxides*, 1st edn. Academic Press, New York
4. Badwal SPS (1984) *J Mater Sci* 19:1767. doi:[10.1007/BF00550246](https://doi.org/10.1007/BF00550246)
5. Ioffe AI, Rutman DS, Karpachov SV (1978) *Electrochim Acta* 23:141. doi:[10.1016/0013-4686\(78\)80110-8](https://doi.org/10.1016/0013-4686(78)80110-8)
6. Pornprasertsuk R, Ramanarayanan P, Musgrave CB, Prinz FB (2005) *J Appl Phys* 98:103513. doi:[10.1063/1.2135889](https://doi.org/10.1063/1.2135889)
7. Meyer M, Nicoloso N, Jaenisch V (1997) *Phys Rev B* 56:5961. doi:[10.1103/PhysRevB.56.5961](https://doi.org/10.1103/PhysRevB.56.5961)
8. Shimojo F, Okazaki H (1992) *J Phys Soc Jpn* 61:4106. doi:[10.1143/JPSJ.61.4106](https://doi.org/10.1143/JPSJ.61.4106)
9. Yamamura H, Utsunomiya N, Mori T, Atake T (1998) *Solid State Ionics* 107:185. doi:[10.1016/S0167-2738\(97\)00534-1](https://doi.org/10.1016/S0167-2738(97)00534-1)
10. Filal M, Petot C, Mokchah M, Chateau C, Carpentier JL (1995) *Solid State Ionics* 80:27. doi:[10.1016/0167-2738\(95\)00137-U](https://doi.org/10.1016/0167-2738(95)00137-U)
11. Gibson IR, Irvine JTS (1996) *J Mater Chem* 6:895. doi:[10.1039/jm9960600895](https://doi.org/10.1039/jm9960600895)
12. Strickler DW, Carlson WG (1964) *J Am Ceram Soc* 47:122. doi:[10.1111/j.1151-2916.1964.tb14368.x](https://doi.org/10.1111/j.1151-2916.1964.tb14368.x)
13. Irvine JTS, Feighery AJ, Fagg DP, Garcia-Martin S (2000) *Solid State Ionics* 136:879. doi:[10.1016/S0167-2738\(00\)00568-3](https://doi.org/10.1016/S0167-2738(00)00568-3)
14. Dixon JM, LaGrange LD, Merten U, Miller CF, Porter JT II (1963) *J Electrochem Soc* 110:276. doi:[10.1149/1.2425731](https://doi.org/10.1149/1.2425731)
15. Irvine J, Gibson I, Fagg D (1995) *Ionics* 1:279. doi:[10.1007/BF02390208](https://doi.org/10.1007/BF02390208)
16. Weller M, Herzog R, Kilo M, Borchardt G, Weber S, Scherrer S (2004) *Solid State Ionics* 175:409. doi:[10.1016/j.ssi.2003.12.044](https://doi.org/10.1016/j.ssi.2003.12.044)
17. Goodenough JB (2003) *Annu Rev Mater Res* 33:91. doi:[10.1146/annurev.matsci.33.022802.091651](https://doi.org/10.1146/annurev.matsci.33.022802.091651)
18. Lee TA, Navrotsky A, Molodetsky I (2003) *J Mater Res* 18:908. doi:[10.1557/JMR.2003.0125](https://doi.org/10.1557/JMR.2003.0125)
19. Navrotsky A, Benoist L, Lefebvre H (2005) *J Am Ceram Soc* 88:2942
20. Shannon RD (1976) *Acta Crystallogr A* 32:751. doi:[10.1107/S0567739476001551](https://doi.org/10.1107/S0567739476001551)
21. Martin M (2006) *J Electroceram* 17:765. doi:[10.1007/s10832-006-6007-z](https://doi.org/10.1007/s10832-006-6007-z)
22. Almond DP, West AR (1987) *Solid State Ionics* 23:27. doi:[10.1016/0167-2738\(87\)90078-6](https://doi.org/10.1016/0167-2738(87)90078-6)